Indian Journal of Chemistry
Vol. 56A, July 2017, pp. 780-785

Sulphur and cerium co-doped mesoporous titanium dioxide photocatalysts and their photocatalytic activity in the degradation of methylene orange

Zelin Niu[a], Zhanping Song[a, *], Jingping Qiu[b], Xiaogang Sun[b] & Jun Xing[b]

[a]College of Civil Engineering, Xi'an University of Architecture and Technology, Xi'an 710055, China
Email: szp1916@sina.com

[b]Key Laboratory of Ministry of Education on Safe Mining of Deep Metal Mines, Northeastern University, Shenyang 110819, China

Received 20 April 2016; revised and accepted 30 June 2017

A series of sulphur and cerium co-doped mesoporous titanium dioxide photocatalysts have been prepared by a template method using thiourea, ammonium ceric nitrate and tetrabutyl titanate as precursors and Pluronic P123 as a template. The morphology, crystal structure, surface structure and optical absorption properties of the prepared samples are characterized by scanning electron microscopy, X-ray diffraction, N_2 adsorption-desorption measurements and UV-vis absorption spectra. The microcrystal of the co-doped photocatalyst comprises the anatase phase. Compared with mesoporous titanium dioxide, the co-doped samples extends the photoabsorption edge into the visible light region. The photocatalytic activities of the obtained photocatalysts under UV and visible light have been estimated by measuring the degradation rate of methylene orange in aqueous solution. Results show that the co-doped mesoporous titanium dioxide exhibits higher photocatalytic activity than mesoporous titanium dioxide under light irradiation. The synergistic effect of sulphur and cerium co-doping plays an important role in improving the photocatalytic activity.

Keywords: Photocatalysts, Mesoporous catalysts, Doping, Co-doping, Cerium doping, Sulphur doping, Degradation, Methylene orange degradation, Titanium dioxide

Titanium dioxide (TiO_2) is a semiconductor photocatalyst widely used in environmental applications because of its availability at low cost, non-toxicity and biocompatibility, especially for the decomposition of gaseous[1–3] and liquid phases[4–7]. Compared with TiO_2, mesoporous TiO_2, which displays better photocatalytic activity because of its high specific surface area and uniform pore diameter, has received much interest in photocatalysis[8,9]. However, in field applications, there are at least one obvious problems arising from using fine mesoporous TiO_2, i.e., the low photoefficiency of pure mesoporous TiO_2. In order to improve the photocatalytic activity of fine TiO_2 powders, many studies[10-12] have been carried out, which showed that selective metal ion doping can extend the light absorption toward the visible light range and prohibit the recombination of electron-hole pairs of this material, and hence raise photocatalytic performance.

Rare earth metals having incompletely occupied 4*f* and empty 5*d* orbitals often serve as catalyst or catalysis promoter. Studies[13-16] have shown that the photocatalytic activity of TiO_2 can be improved by the doping of some rare earth metals. Also, it has been proved that cerium, as one of the rare earth metals, has the ability to improve the photocatalytic activity of TiO_2[17-20]. Asahi *et al*.[10] first reported the N-doped TiO_2 photocatalyst exhibiting photoabsorption at wavelengths longer than 400-nm and photocatalytic activity under visible light. From there on, some researchers paid much attention to the modification of TiO_2 by incorporating nonmetals, such as phosphorous[21], sulphur[22], fluorine[23], boron[24], carbon[25]. Furthermore, there were also a few reports on TiO_2 photocatalysts co-doped by two kinds of nonmetals[26, 27]. Obviously, doping with these nonmetals can decrease the band gap and result in the response to the visible light of photocatalysts. However, to the best of our knowledge, co-doping of sulphur and cerium in mesoporous TiO_2 powders and their catalytic properties have not been reported so far. In this paper, a series of S, Ce co-doped mesoporous TiO_2 photocatalysts were prepared by a template method using tetrabutyl titanate, thiourea and ammonium ceric nitrate as the sources of Ti, S and Ce, and Pluronic P123 as template. The photocatalytic activity of the prepared samples was evaluated by photodegradation of methyl orange (MO) over the obtained samples under UV and visible light irradiation. Moreover, the effect of co-doping on the photocatalytic activity of mesoporous TiO_2 was investigated and the activity of mesoporous TiO_2 was increased by doping with sulphur and cerium. It can therefore be potentially applied for the treatment of water contaminated by dye pollutants.

Experimental

All the chemicals used in this study are of analytical grade. All the solutions in the study were prepared

using deionized water. All glassware was cleaned by rinsing with hydroxylamine hydrochloride, soaking in 10% HCl, and rinsing with deionized water. The photocatalysts used in this study were synthesized using a slightly modified procedure from that reported in the literature[20]. The prepared samples were labeled as S_xCe_y-$MTiO_2$, where x and y correspond to the initial mole ratios of S to Ti and Ce to Ti, respectively.

The specific surface area and pore volumes of samples were obtained by nitrogen adsorption-desorption at 77 K using the BET method[28] with a Micromeritics 2000 instrument (ASAP 2000, Micromeritics, USA). Scanning electron microscopy (SEM) micro-images of pure $MTiO_2$ and $S_{0.02}Ce_{0.01}MTiO_2$ were obtained on a Philips XL-30 (25 kV, LaB6 filament) scanning electron microscope. The crystalline phases of the prepared samples were identified by X-ray diffraction. The XRD patterns were recorded in the range of 2θ = 20-80° by step scanning with a Rigaku D/max-r B X-ray diffractometer using graphite monochromatic copper radiation (Cu-Kα) at 45 kV, 40 mA. UV-vis absorption spectroscopic measurements were made using a UV-vis diffuse reflectance spectrophotometer (Shimadzu UV-2550). Reflectance spectra were referenced to $BaSO_4$. The band gap energies (Eg) of the prepared photocatalysts can be calculated by the formula Eg = 1239.8/λg from the wavelength values corresponding to the intersection point of the vertical and horizontal parts of the spectra (λg)[29].

The photocatalytic activity of the prepared catalysts under UV and visible light was estimated by measuring the degradation rate of MO (20 mg/L) in an aqueous solution without concerning the degradation intermediates in detail. The photoreaction under UV light was carried out using a magnetically stirred quartz reactor and an ultraviolet mercury lamp (150 W, 365 nm) at about 20 °C. Sixty-minute adsorption time in dark condition was allowed before the start of photoreactions. Then, samples of the suspension were withdrawn after a definite time interval and filtered through 0.22 μm filter paper. The filtrates were analyzed for residual MO concentration using a UV-vis spectrophotometer (UV762, Shanghai Analysis Co.). For comparison, the pure $MTiO_2$ prepared by the same method was used as reference systems. All the experiments were carried out in triplicate. The results presented are the mean values with a total error of less than 5%.

The experiment with visible light irradiation was performed at about 20 °C by using a 150 W metal halide lamp as the light source. In order to limit the irradiation wavelength, the light beam was passed through a 410-nm cut filter (L41) to assure cut-off wavelengths shorter than 410 nm. Then, samples of the suspension were withdrawn after a definite time interval and filtered through 0.22 μm filter paper to analyze the residual MO concentration.

Results and discussion

SEM images of pure $MTiO_2$ and $S_{0.02}Ce_{0.01}$-$MTiO_2$ are shown in Fig. 1. It can be seen that particles of pure $MTiO_2$ congregated together so densely that few gaps exist between the pores. In contrast, the particles of $S_{0.02}Ce_{0.01}$-$MTiO_2$ sample congregated loosely. This may be due to the positive effect of S and Ce on $MTiO_2$ since the S and Ce co-doping not only increased the surface area but also increased the pore volume of $MTiO_2$ catalyst. It can be observed that samples were present in the form of the approximately spherical particle.

To obtain information on the crystal structure of the prepared photocatalysts, their X-ray diffraction

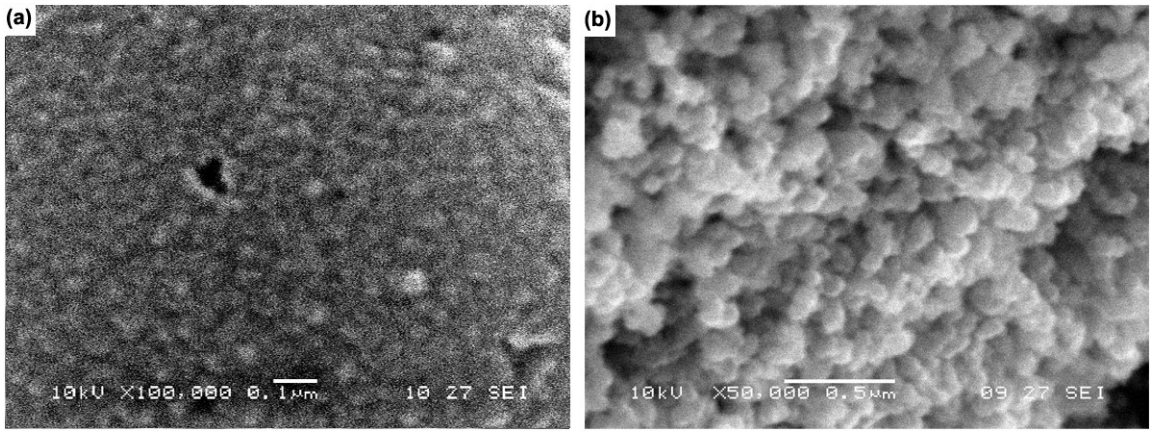

Fig. 1 – SEM images of different samples. (a) pure $MTiO_2$, and (b) $S_{0.02}Ce_{0.01}$-$MTiO_2$.

patterns were recorded. The XRD patterns of prepared samples were shown in Fig. 2. It is observed that all prepared $MTiO_2$ powders were present in the anatase phase and that there is no evident difference between anatase $MTiO_2$ and doped $MTiO_2$. The diffraction peaks at 25.38°, 37.80°, 48.05°, 55.07° and 70.25° are consistent with the (1 0 1), (0 0 4), (2 0 0), (1 0 5) and (2 2 0) peaks of anatase TiO_2. The XRD results suggest that the S and Ce doping has little influence on the nature of crystal formation.

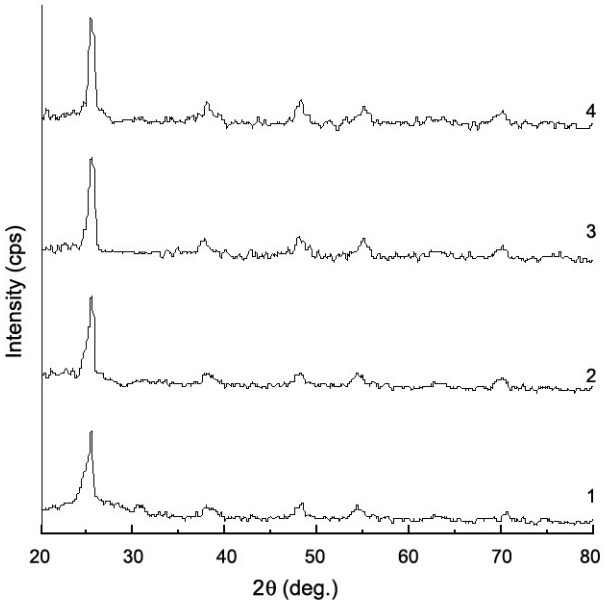

Fig. 2 – XRD patterns of different samples. [(1) pure $MTiO_2$; (2) $S_{0.02}$-$MTiO_2$; (3) $Ce_{0.01}$-$MTiO_2$; (4) $S_{0.02}Ce_{0.01}$-$MTiO_2$].

The BET surface area and pore volume of prepared catalysts are summarized in Table 1. The measured BET surface areas of doped samples are higher than that of pure $MTiO_2$; the $S_{0.02}Ce_{0.01}$-$MTiO_2$ sample displayed the highest specific surface area of 185 $m^2\ g^{-1}$ and the highest pore volume of 0.383 $cm^3 \cdot g^{-1}$. The N_2 adsorption-desorption isotherms and Barret-Joyner-Halenda (BJH) pore size distribution plots (calculated from the adsorption branch) of pure $MTiO_2$ and $S_{0.02}Ce_{0.01}$-$MTiO_2$ are shown in Fig. 3. The adsorption-desorption isotherms of all samples are of type IV with H2 hysteresis loop[30] with stepwise adsorption and desorption. The sharp decline in the desorption curve and the hysteresis loop at high relative pressure are indicative of mesoporosity. The larger are the sample pore sizes, the higher the pressure of capillary cohesion that occurred[31]. As shown in Fig. 3, the capillary cohesion of mesoporous TiO_2 occurs at higher pressure and that of $S_{0.02}Ce_{0.01}$-$MTiO_2$ occurs at lower pressure.

Table 1 — Physicochemical properties of the prepared samples

Sample	S_{BET} (m^2/g)	Total pore vol. (cm^3/g)	Band gap (eV)
$MTiO_2$	165	0.361	3.22
$S_{0.02}$-$MTiO_2$	173	0.365	3.11
$Ce_{0.01}$-$MTiO_2$	181	0. 372	2.97
$S_{0.02}$ $Ce_{0.01}$-$MTiO_2$	185	0.383	2.88

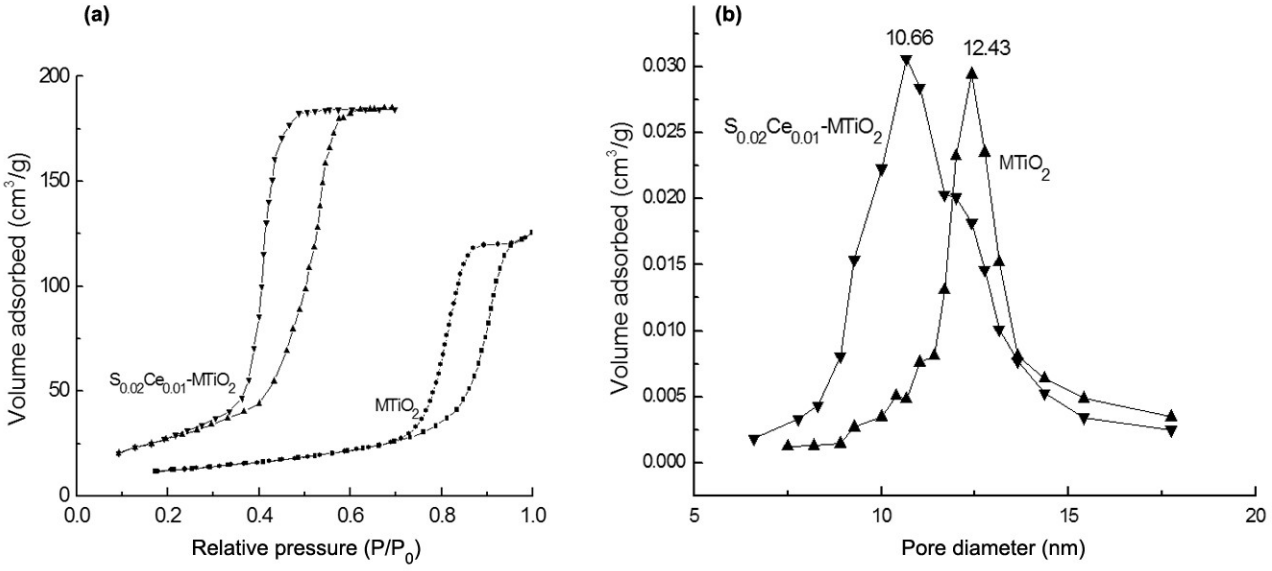

Fig. 3 – (a) N_2 adsorption-desorption isotherms of samples, and, (b) BJH pore size distributions of samples.

It suggests that mesoporous TiO_2 has larger pore size and $S_{0.02}Ce_{0.01}$-$MTiO_2$ has smaller pore size. The narrow pore size distribution range indicates that the present materials have uniform pore channels and most pores have a diameter of about 10.0-13.0 nm.

UV-vis absorption spectra were recorded to characterize the light absorption ability of the prepared photocatalysts (Fig. 4). The UV-vis absorption spectra show the influence of S, Ce doping on the UV-vis absorption. Modification of $MTiO_2$ with S and Ce significantly affected the absorption properties of photocatalysts. The absorption in the region between 420 and 700 nm for the single doped and co-doped photocatlysts is shifted to a longer wavelength as compared to pure $MTiO_2$. Modification of S and Ce caused the absorption spectra of the samples to shift to the visible region demonstrating that S and Ce co-doping was in favor of visible light absorption. This extended absorbance indicates the possible enhancement in the photocatalytic activity of $MTiO_2$ illuminated by visible light. The band gap energies (Eg) of the prepared photocatalysts calculated by the formula $Eg = 1239.8/\lambda g$ are listed in Table 1. For pure $MTiO_2$ prepared without any dopant, the Eg was 3.22 eV. In the case of doped $MTiO_2$, Eg decreased from 3.11 to 2.88 eV. The lowest Eg (2.88 eV) was observed for sample $S_{0.02}Ce_{0.01}$-$MTiO_2$ (see Table 1). The narrowing of band gaps of the prepared doped $MTiO_2$ suggests that they should be possibly responsive to the visible light.

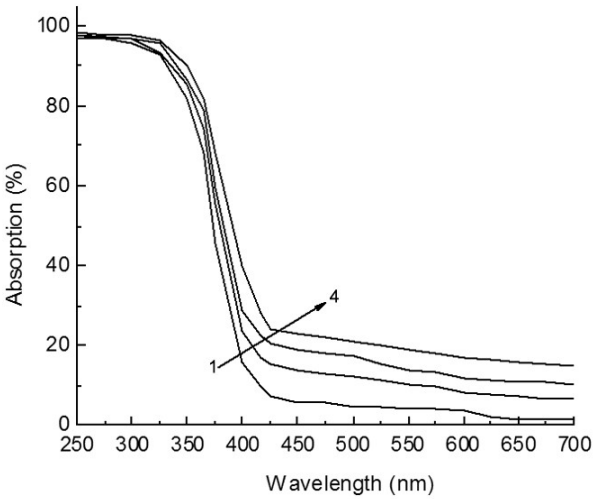

Fig. 4 – UV-vis absorption spectra of different samples. [(1) pure $MTiO_2$; (2) $S_{0.02}$-$MTiO_2$; (3) $Ce_{0.01}$-$MTiO_2$; (4) $S_{0.02}Ce_{0.01}$-$MTiO_2$].

Photocatalytic activities of S and Ce co-doped $MTiO_2$ samples were estimated by measuring the degradation rate of MO (20 mg/L) without focusing on the degradation intermediates in detail. Pure $MTiO_2$, S-doped and Ce-doped $MTiO_2$ synthesized by the same method were used as the reference systems.

Figure 5(a) shows the results of MO degradation with irradiation time under UV light irradiation in the presence of S and Ce co-doped $MTiO_2$ photocatalysts. It is observed that all as-prepared samples exhibit higher photocatalytic activity than pure $MTiO_2$ and single-doped $MTiO_2$ under UV light. It is also seen that the co-doped content had an effect on the degradation ratios. Among the samples, the best performance was attributed to $S_{0.02}Ce_{0.01}$-$MTiO_2$. Results show that the

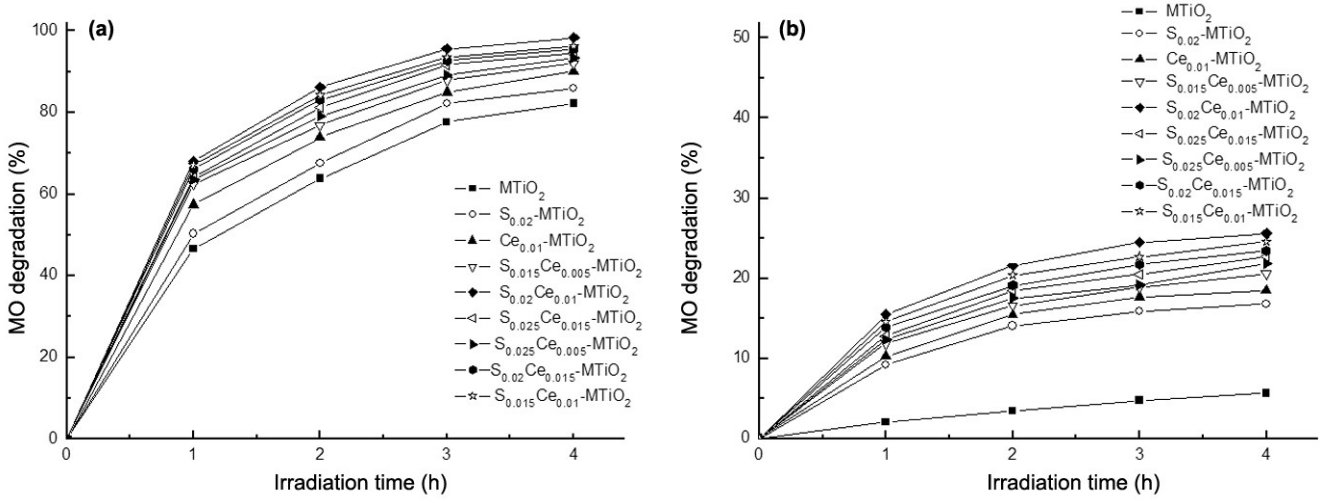

Fig. 5 – Degradation curves of MO under (a) UV light and (b) visible light with varying irradiation time. [Initial conc. of MO: 20 mg/L; catalyst: 1.0 g/L; calcination temp.: 500 °C)].

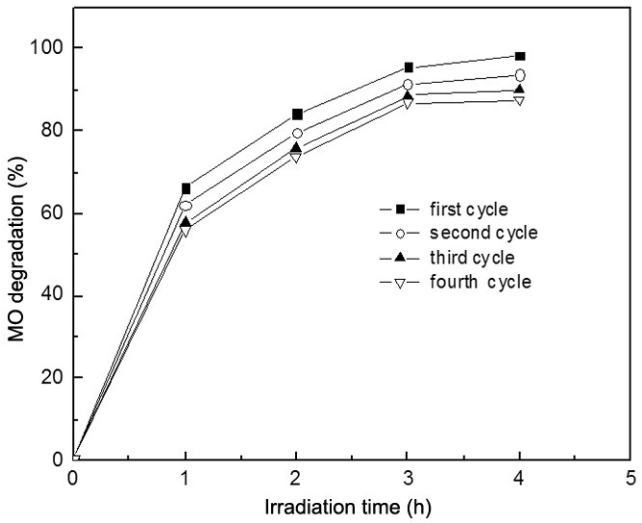

Fig. 6 – Recyclability of $S_{0.02}Ce_{0.01}$-$MTiO_2$ under UV light.

photocatalytic performance of $S_{0.02}Ce_{0.01}$-$MTiO_2$ was almost twice as that of pure $MTiO_2$ for degradation of MO under UV light. This result may be due to the positive effect of the introduction of S and Ce on the photocatalytic activity because the co-doping not only increased the surface area of $MTiO_2$ but also extended its photoabsorption to visible light region. In addition, the rare earth metals which usually act as a reservoir for photogenerated electrons, promote an efficient charge separation in doped TiO_2 photocatalysts, which improved the photocatalytic activity of S and Ce co-doped $MTiO_2$. The surface area is one of the key factors to control the photocatalytic activity of the photocatalyst. The larger the surface area is, the higher the photocatalytic activity is. Furthermore, the photoabsorption characters greatly affect the photocatalytic activity of a photocatalyst, since the numbers of absorbed photons directly depend on the absorption property of the photocatalyst. From the UV-vis absorption spectra of samples (Fig. 4), it may be seen that the intensity and region of visible light photoabsorption on S and Ce co-doped $MTiO_2$ was stronger and larger, respectively than those of pure $MTiO_2$. Obviously, the photocatalytic activity of S and Ce co-doped $MTiO_2$ under UV light demonstrated that S and Ce co-doping effects were exceptional. This may be ascribed to the cooperative effects of S and Ce co-doping.

Photocatalytic activities of different samples under visible light were shown in Fig. 5(b). It could be observed that all doped samples exhibited photocatalytic activity under visible light. Among the studied samples, $S_{0.02}Ce_{0.01}$-$MTiO_2$ showed the best photocatalytic performance corresponding to the maximum red shift in the UV-vis diffusive reflectance absorption spectra (Fig. 4). The photocatalytic performance of $S_{0.02}Ce_{0.01}$-$MTiO_2$ was almost 4.0 times higher than that of pure $MTiO_2$ for degradation of MO under visible light, which was in agreement with the outcome from the optical absorption spectra analysis.

In order to test recyclability of $S_{0.02}Ce_{0.01}$-$MTiO_2$ photocatalyst, the photocatalytic degradation experiments of MO were repeated for four cycles (Fig. 6). It was observed that the photocatalytic activity of the present photocatalyst was only slightly reduced in stirred aqueous solution up to four cycles. The photocatalytic activity of $S_{0.02}Ce_{0.01}$-$MTiO_2$ remained *ca*. 87.9% of the activity of the as-prepared sample after being used four times; the degradation percentage of MO reached 86.5% when irradiation time was 4 h. This indicates that the final removal of MO from solutions is caused by the photocatalytic degradation rather than the adsorption process that leads to saturated adsorption of MO on the photocatalyst. These results indicate that cyclic usage of $S_{0.02}Ce_{0.01}$-$MTiO_2$ was possible and its stability in treating polluted water was satisfactory. Therefore, it shows potential for continuous photocatalytic degradation processes.

In conclusion, in the present study, a composite photocatalyst of S and Ce co-doped mesoporous TiO_2 was successfully prepared by template method using thiourea, ammonium ceric nitrate and tetrabutyl titanate ($Ti(OC_4H_9)_4$) as precursors and Pluronic P123 as template. The photocatalyst thus prepared was applied to degrade contaminated water of MO. The as-prepared photocatalyst contained only the anatase phase. S and Ce co-doping caused absorption spectra of mesoporous TiO_2 to shift to the visible region. The results showed that S and Ce co-doping enhance the photocatalytic activity of $MTiO_2$ under UV and visible light irradiation, and that $S_{0.02}Ce_{0.01}$-$MTiO_2$ exhibits the optimum photocatalytic activity for MO degradation. The synergistic effect of S and Ce co-doping was responsible for improving the photocatalytic performance.

Acknowledgment

The authors deeply appreciate the support from the National Natural Science Foundation of China (51578447) and Shaanxi province Department of Education Foundation of China, (16JK1443), and funds from Shaanxi province Housing Urban and Rural Construction Technology Research and Development Project Foundation of China (2016-K4-021).

References

1 Ao C H, Lee S C, Yu Y Z & Xu J H, *Appl Catal B*, 54 (2004) 41.
2 Fujishima A, Rao T N & Tryk D A, *J Photochem Photobiol C*, 1 (2000) 1.
3 Strini A, Cassese S & Schiavi L, *Appl Catal B*, 61 (2005) 90.
4 Rodrigues A C, Boroski M, Shimada N S, Garcia J C, Nozaki J & Hioka N, *J Photochem Photobiol A,* 194 (2008) 1.
5 Thompson T L & Yates J T, *Chem Rev*, 106 (2006) 4428.
6 Jiang D, Zhao H, Zhang S & John R, *J Catal*, 223 (2004) 212.
7 Yao S, Li J & Shi Z, *Particuology*, 8 (2010) 273.
8 Yu J, Su Y, Cheng B & Zhou M, *J. Mol Catal A*, 258 (2006) 104.
9 Koshitani N, Sakulkhaemaruethai S, Suzuki Y & Yoshikawa S, *Ceramics Int*, 32 (2006) 819.
10 Asahi R, Morikawa T, Ohwaki T, Aoki K & Taga Y, *Science*, 293 (2001) 269.
11 Sun B, Reddy E P & Smirniotis P G, *Appl Catal B*, 57 (2005) 139.
12 Xu J, Lu M, Guo X & Li H, *J Mol Catal A*, 226 (2005)123.
13 Ökte A N & Özge Y, *Appl Catal B,* 85 (2008) 92.
14 Xu A W, Gao Y & Liu H Q, *J Catal,* 207 (2002) 151.
15 Baiju K V, Sibu C P, Rajesh K, Krishna Pillai P, Mukundan P, Warrier K G K & Wunderlich W, *Mater Chem Phys,* 90 (2005) 123.
16 Shi Z L, Lai H, Yao S H & Wang S F, *Chin J Chem Phys,* 25 (2012) 96.
17 Xie Y & Yuan C, *Appl Catal B*, 46 (2003)251.
18 Liu Z L, Guo B, Hong L & Jiang H, *J Phys Chem Solids*, 66 (2005) 161.
19 Yao S H, Yang Y, Song S P & Shi Z L, *Indian J Chem*, 53A (2014) 665.
20 Shi Z, Lai H, Yao S & Wang S, *J Chinese Chem Soc,* 59 (2012) 614.
21 Lin L, Zheng R Y, Xie J L, Zhu Y X & Xie Y C, *Appl Catal B*, 76 (2007) 196.
22 Shi Z L, Liu G Q, Sun N, Yao S H & Wang S F, *Russ J Phys Chem A*, 87 (2013) 1300.
23 Yu J C, Yu J G, Ho W K, Jiang Z T & Zhang L Z, *Chem Mater*, 14 (2002) 3808.
24 Zhao W, Ma W H, Chen C C, Zhao J C & Shuai Z G, *J Am Chem Soc*, 126 (2004) 4782.
25 Sakthivel S & Kisch H, *Angew Chemie Int Edn*, 42 (2003) 4908.
26 Wang J, Yin S, Komatsu M & Sato T, *J Eur Ceram Soc*, 25 (2005) 3207.
27 Zhang Z, Wang C, Zakaria R & Ying J Y, *J Phys Chem B*, 102 (1998) 10871.
28 Gregg S J & Sing K S W, *Adsorption, Surface Area and Porosity*, 2nd Edn, (Academic Press, London) 1982.
29 Körösi L & Dékány I, *Colloids Surf A*, 280 (2006) 146.
30 Rojas F, Kornhauser I, Felipe C, Esparza J M, Cordero S, Dominguez A & Riccardo J L, *Phys. Chem Chem Phys*, 4 (2002) 2346.
31 Li D & Haneda H, *J Photochem Photobiol A*, 160 (2003) 203.